



Generation of attenuation map for MR-based attenuation correction of PET data in the head area employing 3D short echo time MR imaging

Parisa Khateri^{a,b}, Hamidreza Salighe Rad^{a,b,*}, Anahita Fathi^b, Mohammad Reza Ay^{a,b,c}

^a Department of Medical Physics and Biomedical Engineering, Tehran University of Medical Sciences, Tehran, Iran

^b Medical Imaging Systems Group, Research Center for Molecular and Cellular Imaging, Tehran University of Medical Sciences, Tehran, Iran

^c Research Institute for Nuclear Medicine, Tehran University of Medical Sciences, Tehran, Iran

ARTICLE INFO

Available online 27 August 2012

Keywords:

PET/MRI

Attenuation correction

Brain imaging

Ultra-short echo-time (UTE) MRI

Short echo-time (STE) MRI

ABSTRACT

Attenuation correction is a crucial step to get accurate quantification of Positron Emission Tomography (PET) data. An attenuation map to provide attenuation coefficients at 511 keV can be generated using Magnetic Resonance Images (MRI). One of the main steps involved in MR-based attenuation correction (MRAC) of PET data is to separate bone from air. Low signal intensity of bone in conventional MRI makes it difficult to separate bone from air in the head area, while their attenuation coefficients are very different. In literature, several groups proposed ultrashort echo-time (UTE) sequences to differentiate bone from air [4,5,7], because these sequences are capable of imaging tissues with short $T2^*$ relaxation time, such as cortical bone; however, they are difficult to use, expensive and time-consuming. Employing short echo-time (STE) MRI in combination with long echo-time (LTE) MRI, and along with high performance image processing algorithms is a good substitute for UTE-based PET attenuation correction; they are widely available, easy to use, inexpensive and much faster than UTE pulse sequences. In this work, we propose the use of STE sequences along with LTE ones, as well as a dedicated image processing method to differentiate bone from air cavities in the head area by creating contrast between the tissues. Attenuation coefficients at 511 keV, relying on literature [5], will then be assigned to the voxels. Acquisition was performed on a clinical 3T Tim Trio scanner (Siemens Medical Solution, Erlangen, Germany), employing a dual echo sequence. To achieve an optimized protocol with the best result for discrimination of bone and air, two types of acquisitions were performed, with and without fat suppression; the acquisition parameters were as follows: TE=1.21/5 ms, TR=5/17, FA=30, and TE=1.12/3.16 ms, TR=5/5, FA=12 for non-fat-suppressed and fat-suppressed protocol, respectively. Contrast enhancement and tissue segmentation were applied as processing steps, to successfully classify voxels into bone, air and soft tissue classes, yielding accuracy, sensitivity and specificity of 88%, 77% and 94%, for non-fat suppressed acquisition, respectively. This method could potentially be as an efficient method for generation of attenuation map in 511 keV for MR-based attenuation correction of PET data in clinical PET/MR applications with mixed air and bone signals.

© 2012 Elsevier B.V. All rights reserved.

1. Introduction

Recently there have been general interests toward hybrid medical imaging systems to combine different imaging modalities for one specific application. Combining PET and MRI in this domain is prominent since it takes advantage of high sensitivity of PET along with versatile contrast mechanisms of MRI in different functional and structural modalities [1]. In combined PET/MRI systems, PET data is intrinsically aligned with anatomical information from MRI, to make it accurate for quantification purposes. Quantification is then improved by using the MRI

information during the attenuation correction (AC) of the PET data [2]. Combined PET/MRI offers several advantages over PET/CT: MRI provides better soft-tissue contrast than CT and the radiation dose to the patient is significantly lower; furthermore, other applications such as spectroscopy or functional MR (fMRI) are also possible with MRI [1].

Reliable AC methods for 3D quantitative PET acquisition require accurate derivation of an attenuation map (μ -map) at 511 keV. The μ -map reflects the tissue attenuation distribution across the imaging volume. The photon attenuation is the direct source of contrast in a CT image, making the use of CT for AC straightforward. This is, however, not a trivial task for the MR images, as they are not directly related to the tissue linear attenuation coefficients. The challenge in MRI-based AC is to develop a method to determine the attenuation coefficients of tissues at 511 keV from a set of MR images.

* Corresponding author at: Department of Medical Physics and Biomedical Engineering, Tehran University of Medical Sciences, 16 Azar, Poor Sina Tehran, Tehran, Iran.

E-mail address: hamid.saligheh@gmail.com (H. Salighe Rad).

Different approaches to determine the μ -map from MR images have been described in the literature [2–7]. These approaches are divided into two main categories: template-based and segmentation-based methods [1]. A problem with template-based methods is that they show significant variability in patient anatomy, for example, in the ethmoidal sinuses in the skull, while, with segmentation-based methods, anatomic variability could be identified and assignment of

corresponding linear attenuation coefficient to different tissues leads to a more relevant attenuation map.

Combining PET with MRI is challenging because of low signal intensity of cortical bone in conventional MRI. The low signal intensity of cortical bone makes it difficult to differentiate bone tissue from air cavities, while there is a significant difference between the attenuation properties of bone and air.

Table 1

Acquisition parameters with and without fat suppression.

Scan parameters (units)		Repetition time (ms)	Echo time (ms)	Flip angle	Pixel bandwidth (Hz/pixel)	Field of view (mm)	Acquisition matrix	Voxel size (mm)
Without fat suppression	LTE	17	5	30	238	350 × 350	512 × 512	0.68 × 0.68 × 2
	STE	5	1.21	30	814			
With fat suppression	LTE	5	3.16	12	651	280 × 280	320 × 320	0.88 × 0.88 × 0.88
	STE	5	1.12	12	651			



Fig. 1. Representative slices from MRI datasets obtained by step by step image processing. (Left to right) STE image, LTE image, subtracted result, bone image from thresholding and μ -map.

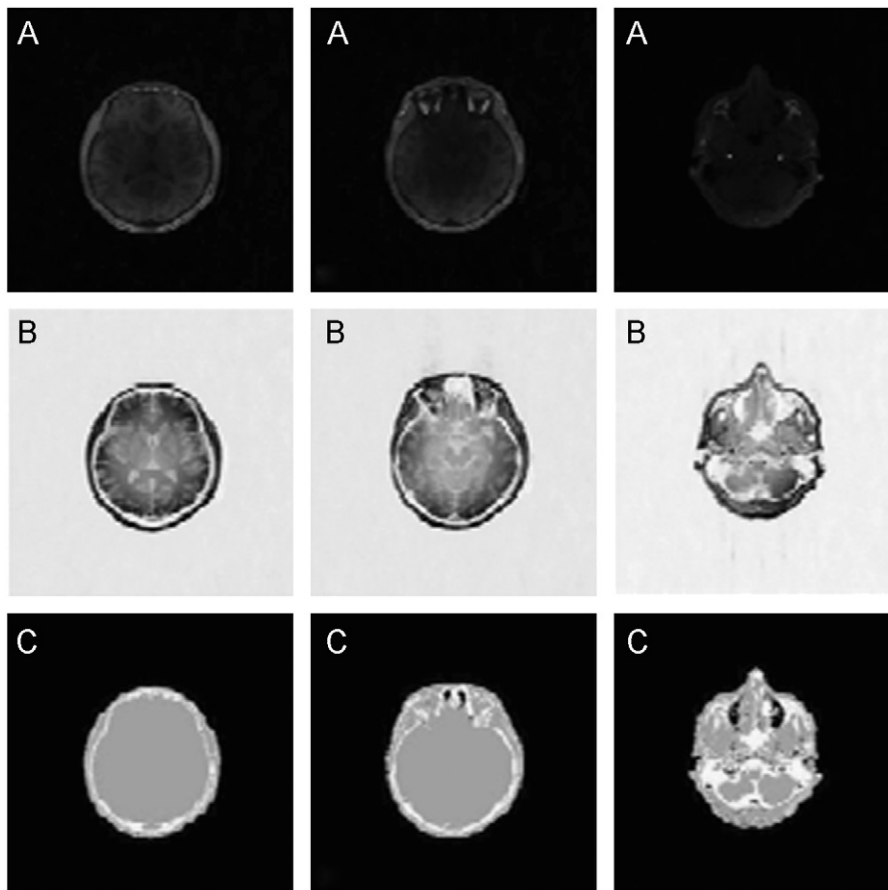


Fig. 2. Visual comparison of transverse slices of different regions for without-fat-suppression data. (A) STE images, (B) difference images and (C) μ -maps. Bone is depicted in white, soft tissue in gray, and air in black in μ -maps.

Recently, a new approach to detect bone signal using ultra-short echo-time (UTE) sequences has been described [4,5,7]. Although UTE sequences have been shown to be suitable to generate patient specific attenuation map based on MR images, they are difficult to use and expensive. According to the value of relaxation time for bone tissue, i.e. $T2^* \approx 700 \mu\text{s}$ at 3 T, since bone signal is also available for a short echo time ($TE \sim 0.5\text{--}1 \text{ ms}$), implementing short echo-time (STE) MRI instead of UTE MRI seems to be a proper alternative for PET-AC; they are widely available on clinical scanners, easy to use, inexpensive, faster than UTE pulse sequences and can be used for dedicated brain PET scanners.

This study aims to investigate the feasibility to employ STE-MRI sequences for generation of μ -map from MR images for attenuation correction of PET data in the head and neck areas. STE MR-based AC was performed as a potential solution to the problem of discriminating air from bone in MR images. For this purpose, MR images with short TE (STE) and long TE (LTE) were acquired, followed by an image processing method to enhance contrast between different tissue classes to yield the μ -map. Finally, clinical applicability of the proposed method was evaluated on MRI brain datasets of 2 patients, one without fat suppression, the other with fat suppression.

2. Materials and methods

2.1. MR acquisition protocol of STE and LTE MR images

The proposed MRI protocol combines STE and LTE acquisitions. The signal from the bone exists in the STE and not in the LTE

acquisition, whereas signals from other tissue classes, i.e., soft tissue and air, are similar in both acquisitions. Since fat and bone tissues are adjacent in most regions of the head, bone signal may be affected by high intensity of fat in STE acquisition. In order to identify the optimal protocol for bone–air discrimination, two series of datasets were acquired, with and without fat suppression.

MR images were acquired on a clinical 3T Tim Trio scanner (Siemens Medical Solution, Erlangen, Germany) using an 8-element head coil. Since the goal of an STE sequence is to visualize bone signal employing commercial scanners with conventional imaging techniques, the echo-time (TE) was chosen to be as short as possible, and about $TE \sim 1 \text{ ms}$ to meet hardware limitations of the system. Scan parameters chosen for these protocols are described in Table 1.

2.2. Generation of the attenuation map at 511 keV

μ -Map was derived by analyzing the data obtained with STE and LTE sequences Fig. 1. Some pre-processing steps were initially applied to improve the identification of three tissue classes: soft tissue, bone and air, to generate the μ -map for the head. These steps were performed in 3D Slicer version 3.6.3 (<http://www.slicer.org>) and MATLAB version 2010a (The MathWorks Inc., Natick, MA, USA). The linear attenuation coefficients assumed for bone, soft tissue and air were 0.143, 0.096 and 0 cm^{-1} , respectively [5].

2.3. Validation strategy

To quantify the accuracy, sensitivity and specificity of the segmentation algorithm, the bone tissue class derived from the

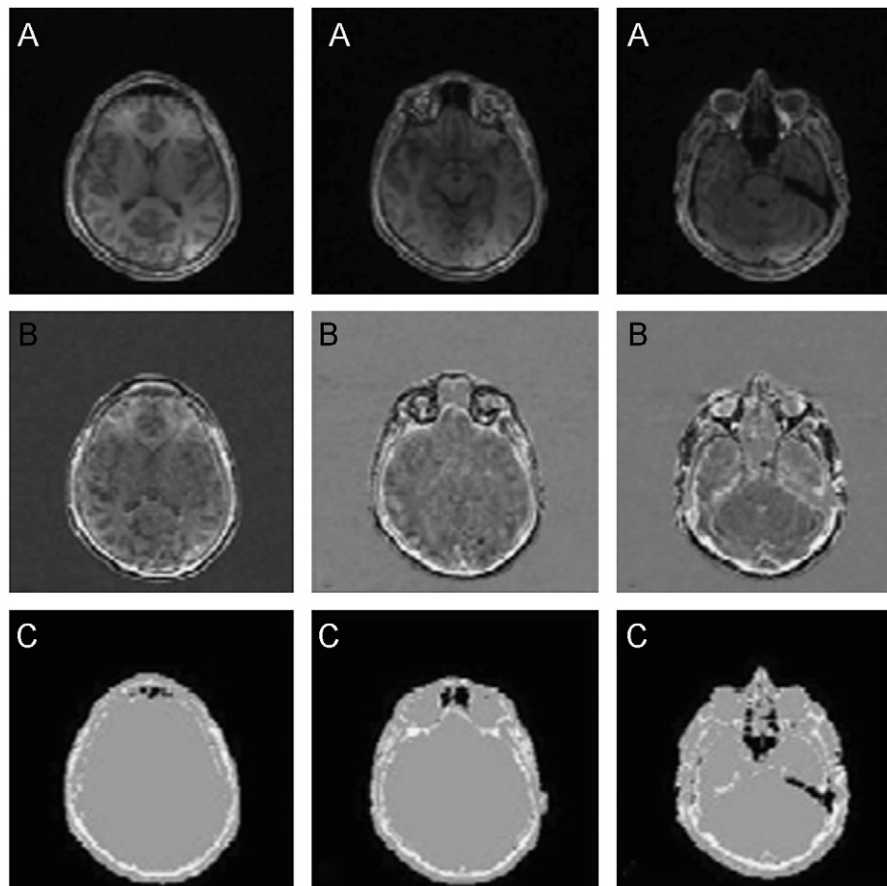


Fig. 3. Visual comparison of transverse slices of different regions for fat-suppressed data. (A) STE images, (B) difference images and (C) μ -maps. Bone is depicted in white, soft tissue in gray, and air in black in μ -maps.

Table 2
SNR of acquired images for bone region, and parameters of quantitative assessment.

Acquisition type		SNR	Accuracy(%)	Sensitivity(%)	Specificity(%)
Without fat suppression	LTE	6	88	77	94
	STE	9			
With fat suppression	LTE	14	79	61	93
	STE	22			

proposed method was compared with the manual segmented MRI, which is segmented by an expert radiologist. Sensitivity, specificity and accuracy were obtained as:

$$\text{Sensitivity} = \frac{TP}{FN+TP} \quad (1)$$

$$\text{Specificity} = \frac{TN}{TN+FP} \quad (2)$$

$$\text{Accuracy} = \frac{TP+TN}{TP+FN+TN+FP} \quad (3)$$

in which TP, TN, FP and FN stand for true positive, true negative, false positive and false negative, respectively.

3. Results

Figs. 2 and 3 show corresponding STE images, difference images and μ -maps determined using segmented data, without and with fat suppressions, respectively, employing identical data-processing workflow and similar thresholds to derive μ -maps in fat suppressed protocol, Fig. 3. STE images without fat suppression lead to misclassification of fat as bone in regions with complex bone structure like Paranasal sinuses. SNR analysis for the bone tissue and in both STE and LTE acquisitions are shown in Table 2, suggesting significant bone signal detection for STE acquisitions. Voxel-wise analysis of the semi-automated and manually segmented bone images and for the case of STE acquisitions without fat suppression yielded the overall accuracy, sensitivity and specificity as given in Table 2, resulting in correct segmentation for the majority of voxels and inaccurate bone segmentation in complex regions such as the ethmoidal sinuses. However, STE acquisitions with fat suppression, shown in Fig. 3, suggest successful detection of sinusoidal regions, with some penalty on the achieved SNR, resulting in misclassification of bone in some parts of the nasal air cavities.

4. Discussions

One of the main advantages of our proposed method over previous MR-based AC methods is that it can easily be applied in clinical MR scanning systems, and for PET inserts for dedicated brain imaging. Although the discrimination is significant rather than conventional MR-based AC, it is clear that some improvements should still be made before the method can be used in a routine clinical practice. A known limitation of this method is the low quality of the acquired images. This low quality can be upgraded by carefully tuning acquisition parameters. It is recognized that our method was validated using manually segmented images and limited data. It would be of important value to evaluate the developed AC method using the CT-based AC method as gold standard, and to assess the reproducibility of the protocol using more data acquisitions.

5. Conclusions

This work demonstrates the feasibility of classification-based MRAC accounting for three different tissue types—cortical bone, air, and soft tissue—by combining the STE MRI sequence with LTE one, as well as dedicated image processing. The good discrimination of tissue types with different attenuation coefficients demonstrates the applicability of the proposed approach in clinical MR systems. The proposed method is still under development and will be clinically validated with large patient population.

Acknowledgments

This work was supported by Tehran University of Medical Sciences, Tehran, Iran, under Grant no. 17017.

References

- [1] H. Zaidi, A. Del Guerra, *Medical Physics* 38 (2011) 5667.
- [2] H. Zaidi, M.L. Montandon, D.O. Slosman, *Medical Physics* 30 (2003) 937.
- [3] A. Martinez-Möller, M. Souvatzoglou, G. Delso, R.A. Bundschuh, C. Chefd'hotel, S.I. Ziegler, N. Navab, M. Schwaiger, S.G. Nekolla, *Journal of Nuclear Medicine* 50 (2009) 520.
- [4] V. Keereman, Y. Fierens, T. Broux, Y. De Deene, M. Lonneux, S. Vandenberghe, *Journal of Nuclear Medicine* 51 (2010) 812.
- [5] C. Catana, A. van der Kouwe, T. Benner, C.J. Michel, M. Hamm, M. Fenchel, B. Fischl, B. Rosen, M. Schmand, A.G. Sorensen, *Journal of Nuclear Medicine* 51 (2010) 1431.
- [6] I.B. Malone, R.E. Ansorge, G.B. Williams, P.J. Nestor, T.A. Carpenter, T.D. Fryer, *Journal of Nuclear Medicine* 52 (2011) 1142.
- [7] Y. Berker, J. Franke, A. Salomon, M. Palmowski, H.C.W. Donker, Y. Temur, F.M. Mottaghy, C. Kuhl, D. Izquierdo-Garcia, Z.A. Fayad, *Journal of Nuclear Medicine* 53 (2012) 796.